Donor states in a multi-layered quantum dot

2000 J. Phys.: Condens. Matter 12 8641

(http://iopscience.iop.org/0953-8984/12/40/308)

J. Phys.: Condens. Matter **12** (2000) 8641–8653. Printed in the UK PII: S0953-8984(00)13020-6

Donor states in a multi-layered quantum dot

Cheng-Ying Hsieh and Der-San Chuu†

Deh Yu College of Nursing and Management, Keelung 203, Taiwan
and
Department of Electrophysics, National Chiao Tung University, Hsinchu 300, Taiwan

E-mail: dschuu@cc.nctu.edu.tw

Received 3 April 2000, in final form 14 August 2000

Abstract. The ground and excited state energies of a hydrogenic impurity located at the centre of a multi-layered quantum dot (MLQD) are calculated in the framework of the effective-mass approximation. The MLQD consists of a spherical core (e.g. GaAs) and a coated spherical shell (e.g. $Ga_{1-x}Al_xAs$). The whole dot is then embedded inside a bulk material (e.g. $Ga_{1-y}Al_yAs$). We solve the Schrödinger equation exactly. The eigenfunctions of the impurity are expressed in terms of Whittaker function and Coulomb wavefunction. The state energies are expressed in terms of the shell thickness, core radius, total dot radius and the potential heights. Our calculation shows that, as the dot radius approaches infinity, the state energies of an impurity located at the centre of a multi-layered or a single-layered QD approach $-1/n^2$ Ry, where n is the principal quantum number, $\mathrm{Ry} = \mu e^4/2\varepsilon^2\hbar^2$, μ and ε are the electronic effective mass and the dielectric constant of GaAs material. Thus it behaves like a three-dimensional free hydrogen atom. For very small dot radius, however, the state energy of the hydrogenic impurity of a MLQD behaves very differently from that of a single-layered QD. For a multi-layered QD with finite shell and bulk potential barrier heights, the state energies of the impurity are found to be dependent on the difference of the shell potential (V_2) and the bulk potential (V_3).

1. Introduction

The development and improvement of semiconductor growth techniques such as chemical vapour deposition (CVD), liquid-phase epitaxy (LPE) and molecular beam epitaxy (MBE) have led to the possibility of controlling material composition and of incorporating impurity on the electronic de Broglie scale [1–5]. Impurity states in various confined systems, such as quantum wells (QWs), quantum-well wires (QWWs) and quantum dots (QDs), have been a subject of extensive investigations in basic and applied research. Quasi-two-dimensional (quasi-2D) quantum wells have been widely studied and applied to various semiconductor devices, such as high-electron-mobility transistors. Quasi-one-dimensional systems, such as quantum-well wires, are known to have the advantage of high mobility and suppression of carrier scattering.

Since Bastard's [6] pioneering work on the study of the binding energy of a hydrogenic impurity within an infinite potential-well structure, many theoretical and experimental works have been devoted to the study of the properties of impurity states in the quantum well, quantum-well wire and quantum dot [6–31]. The binding energy of the ground state of a hydrogenic impurity E_b in D dimensions is given by [23] $E_b = [2/(D-1)]^2$ Ry, where Ry is the effective Rydberg. In the 2D case, the binding energy increases four times relative to the

† Author to whom correspondence should be addressed.

3D case, while in the 1D case the increase is infinite. The binding energies for bound states of a hydrogenic impurity in a quantum-well wire with infinite [10] or finite [11] confining potential have also been studied. The binding energies for the bound states of a hydrogenic impurity in a quantum-well wire of GaAs–$Ga_{1-x}Al_xAs$ have been found to be two to three times larger than those of comparable 2D wells. The neutral acceptor binding energy was determined as a function of the GaAs quantum well width by using the photoluminescent and excitation spectra [12]. The ground state binding energy of the impurity located inside a QWW or a QD has been calculated by many authors [9–11, 14, 15, 19–22, 24–31].

Recently, Bose [25] and Bose and Sarkar [24, 26, 27] studied the binding energy of impurity in the QD with a computational tedious variational method and showed that the simple perturbation method is able to yield fairly accurate results even in the regime of moderate confinement. Betancur and coworkers [28–31] have also calculated the energy states of on-centre donors in the QD with the variational method. All of the previous calculations showed that the binding energy of the impurity atom in a quantum well depends prominently on the barrier height V_0 and the well (dot) size. The physical properties of electrons in quantum dots are very different from those in the bulk. As a consequence of the confinement, energy levels are discrete. The existence of these atomic-like states may be utilized in future lasers where laser properties can be tailored by proper choices of well and barrier materials as well as the sizes and shapes of the QDs. The change in impurity binding energies due to confinement effect has been observed in photoluminescence [12, 32–34] and Raman-scattering [35, 36] experiments on the impurities in the quantum wells. The study of the impurity states in quantum dots is of interest in physics because specific properties of the impurity in lower-dimensional structures can be achieved easily by varying the radius of the quantum dot. Moreover, the effective strength of the Coulomb interaction between the electron and the impurity atom depends on the geometric dimension of the system and is enhanced as the size of the system is reduced. Thus, the effective strength of the Coulomb interaction in QDs can be adjusted by varying the dot radius. On the contrary, dramatic changes in the binding energies may serve as a clear signal for changes in the effective dimension of QDs.

The first attempt to use more than a single quantum well was done by Chaudhuri [37], who used three quantum wells in his variational calculation of the ground state energy of the donor electron with respect to the lowest subband level. Lane *et al* [38] calculated the binding energies and probability distributions of shallow donor states in multiple-well GaAs–$Ga_{1-x}Al_xAs$ heterostructure. Many authors [39–42] used colloidal chemistry techniques and wet chemistry to prepare the CdS/HgS/CdS multiple-well in which a shell of HgS is embedded in a CdS quantum dot, forming a 'quantum-dot quantum well' (QDQW). The homogeneous absorption and fluorescence spectra of QDQW have also been investigated. Numerous studies on organic LEDs have used these structures as the emitting and charge transport species [43–45]. In this work we calculate the ground state binding energy of the hydrogenic impurity located at the centre of the multi-layered quantum dot by using the effective-mass approximation. Our system was constructed as a spherical core made of GaAs surrounded by a spherical shell of $Ga_{1-x}Al_xAs$ and then embedded in the bulk of $Ga_{1-y}Al_yAs$. The polarization and image charge effects [46–48] may be significant in the multi-layered system if there is a large dielectric discontinuity between the dot and the surrounding medium. However, this is not the case for the GaAs–$Ga_{1-x}Al_xAs$ quantum system [49] (the dielectric constant of GaAs–$Ga_{1-x}Al_xAs$ is $13.18–3.12x$); therefore these effects may be ignored safely in our calculation. The barrier height V_0 between GaAs and $Ga_{1-x}Al_xAs$ can be obtained [21] as $0.8729x$ eV from a fixed ratio $Q = 0.7$ of the band-gap discontinuity [49] $\Delta E_g = 1.247x$ eV. In this paper, the effective atomic units are used so that all energies are measured in the units of the effective Rydberg (Ry) and all distances are measured in the units of effective Bohr radius a_0^*. The Ry and a_0^* are

defined as $e^2/2\varepsilon a_0^*$ and $\varepsilon\hbar^2/\mu e^2$, where μ and ε are the electronic effective mass and the dielectric constant of GaAs material and equal to 0.067 m_e and 13.18. Thus, the Ry and a_0^* of our system are equal to 5.2 MeV and 104 Å, respectively. In this work, the effective-mass difference between GaAs and $Ga_{1-x}Al_xAs$ material has been ignored.

2. Theory

Consider a hydrogenic impurity located at the centre of a multi-layered spherical dot confined by spherical potential wells. The confining potential is assumed to be $V_1 = 0$ inside the dot ($r < \boldsymbol{a}$); and V_2 inside the shell ($\boldsymbol{a} \leqslant r < \boldsymbol{b}$), V_3 outside the shell ($r \geqslant \boldsymbol{b}$), where $\boldsymbol{a}$ is the core radius and $\boldsymbol{b}$ is the total dot (core plus shell) radius, therefore $\boldsymbol{b} - \boldsymbol{a}$ is the thickness of the shell. According to the effective-mass approximation, the Hamiltonian of the system can be written as

$$H = -\frac{\hbar^2}{2\mu}\nabla^2 - \frac{e^2}{\varepsilon r} + V(r) \tag{1}$$

where

$$V(r) = \begin{cases} 0 & \text{if } r < a \\ V_2 & \text{if } a \leqslant r < b \\ V_3 & \text{if } r \geqslant b \end{cases} \tag{2}$$

and $V(r)$ is the confining potential, μ and ε are the electronic effective mass and the dielectric constant of the material. The Schrödinger equation expressed in spherical coordinates (r, θ, φ)

$$H\Psi(r, \theta, \varphi) = E\Psi(r, \theta, \varphi) \tag{3}$$

can be written as:

$$-\frac{\hbar^2}{2\mu}\left[\frac{\partial^2}{\partial r^2} + \frac{2}{r}\frac{\partial}{\partial r} + \frac{1}{r^2\sin\theta}\frac{\partial}{\partial\theta}\left(\sin\theta\frac{\partial}{\partial\theta}\right) + \frac{1}{r^2\sin^2\theta}\frac{\partial^2}{\partial\varphi^2}\right]\Psi - \frac{e^2}{\varepsilon r}\Psi + V(r)\Psi = E\Psi. \tag{4}$$

Separate $\Psi(r, \theta, \varphi)$ into a product of three terms $R(r)\Theta(\theta)\Phi(\varphi)$; where $\Theta(\theta)$ can be expressed in terms of the associated Legendre polynomial, and $\Phi(\varphi) = e^{im\varphi}$, $m = 0, \pm1, \pm2, \ldots$. The equation for the radial part $R(r)$ can be obtained as follows:

$$-\frac{\hbar^2}{2\mu}\left(\frac{\partial^2}{\partial r^2} + \frac{2}{r}\frac{\partial}{\partial r} - \frac{L(L+1)}{r^2}\right)R(r) - \frac{e^2}{\varepsilon r}R(r) + V(r)R(r) = ER(r). \tag{5}$$

This equation can be solved in two different situations:

(I) For $r < \boldsymbol{a}$, $V(r) = 0$. Equation (5) can be rewritten as

$$-\frac{\hbar^2}{2\mu}\left(\frac{\partial^2}{\partial r^2} + \frac{2}{r}\frac{\partial}{\partial r} - \frac{L(L+1)}{r^2}\right)R(r) - \frac{e^2}{\varepsilon r}R(r) = ER(r). \tag{6}$$

As the electron is confined inside the core dot, the existence of positive energy bound states is possible, therefore, solutions of the Schrödinger equation can be studied in two energy regions:

(a) For negative-energy, $E < 0$. Define $\alpha_{1a}^2 = -8\mu E/\hbar^2 > 0$, $\xi = \alpha_{1a}r$ and $\lambda_1 = 2\mu e^2/\varepsilon\hbar^2\alpha_{1a}$. Then (6) can be expressed as

$$\frac{\partial^2 R}{\partial\xi^2} + \frac{2}{\xi}\frac{\partial R}{\partial\xi} + \left(-\frac{1}{4} + \frac{\lambda_1}{\xi} - \frac{L(L+1)}{\xi^2}\right)R = 0. \tag{7}$$

If we further write $R(\xi) = \xi^{-1}W(\xi)$, then (7) becomes

$$\frac{\partial^2 W}{\partial \xi^2} + \left(-\frac{1}{4} + \frac{\lambda_1}{\xi} + \frac{\frac{1}{4} - (L+\frac{1}{2})^2}{\xi^2}\right) W = 0. \tag{8}$$

Equation (8) is the Whittaker equation [50, 51] which has two linearly independent solutions:

$$W_{\lambda_1,L}(\xi) = \mathrm{e}^{-\xi/2}\xi^{L+1}\Phi(L+1-\lambda_1, 2L+2, \xi) \tag{9}$$

or

$$W_{\lambda_1,-L}(\xi) = \mathrm{e}^{-\xi/2}\xi^{-L+1}\Phi(-L+1-\lambda_1, -2L+2, \xi) \tag{10}$$

where Φ is the confluent hypergeometric function

$$\begin{aligned}\Phi(a,b,x) &= 1 + \frac{a}{b}\frac{x}{1} + \frac{a(a+1)}{b(b+1)}\frac{x^2}{2!} + \cdots + \frac{a(a+1)\ldots(a+k)}{b(b+1)\ldots(b+k)}\frac{x^k}{k!} + \cdots \\ &= \sum_{k=0}^{\infty}\frac{(a)_k}{(b)_k}\frac{x^k}{k!}.\end{aligned} \tag{11}$$

The solution of equation (7) can be expressed as

$$R(\xi) = \xi^{-1}W_{\lambda_1,L}(\xi) = \mathrm{e}^{-\xi/2}\xi^{L}\Phi(L+1-\lambda_1, 2L+2, \xi) \tag{12}$$

or

$$R(\xi) = \xi^{-1}W_{\lambda_1,-L}(\xi) = \mathrm{e}^{-\xi/2}\xi^{-L}\Phi(-L+1-\lambda_1, -2L+2, \xi). \tag{13}$$

Since the wavefunction has to be finite everywhere, the solution of the radial part in the $r < a$ region can be expressed as

$$R_1(\alpha_{1a}r) = C_{1a}\,\mathrm{e}^{-\alpha_{1a}r/2}(\alpha_{1a}r)^L\Phi(L+1-\lambda_1, 2L+2, \alpha_{1a}r) \tag{14}$$

where C_{1a} is the normalization constant.

(b) For positive-energy, $E > 0$. Define $\alpha_{1b}^2 = 2\mu E/\hbar^2 > 0$, $\xi = \alpha_{1b}r$ and $\beta_1 = -\mu e^2/\varepsilon h^2\alpha_{1b}$, then (6) can be expressed as

$$\frac{\partial^2 R}{\partial \xi^2} + \frac{2}{\xi}\frac{\partial R}{\partial \xi} + \left(1 - \frac{2\beta_1}{\xi} - \frac{L(L+1)}{\xi^2}\right) R = 0. \tag{15}$$

If we further write $R(\xi) = \xi^{-1}F(\xi)$, then (15) becomes

$$\frac{\partial^2 F}{\partial \xi^2} + \left(1 - \frac{2\beta_1}{\xi} - \frac{L(L+1)}{\xi^2}\right) F = 0. \tag{16}$$

Equation (16) is the Coulomb wave equation [52] which has two linearly independent solutions $F_{\beta_1,L}(\xi)$ and $G_{\beta_1,L}(\xi)$, where

$$F_{\beta_1,L}(\xi) = \xi^{L+1}\Phi_{\beta_1,L}(\xi) \tag{17}$$

$$G_{\beta_1,L}(\xi) = F_{\beta_1,L}(\xi)\left(\ln(2\xi) + \frac{q_L(\beta_1)}{p_L(\beta_1)}\right) + \theta_{\beta_1,L}(\xi) \tag{18}$$

and

$$\Phi_{\beta_1,L}(\xi) = \sum_{k=L+1}^{\infty} A_k^L(\beta_1)\xi^{k-L-1}. \tag{19}$$

The recurrence relation can be expressed as:

$$A_{L+1}^L(\beta_1) = 1 \tag{20}$$

$$A_{L+2}^L(\beta_1) = \frac{\beta_1}{L+1} \tag{21}$$

$$A_k^L(\beta_1) = \frac{2\beta_1 A_{k-1}^L(\beta_1) - A_{k-2}^L(\beta_1)}{(k+L)(k-L-1)} \qquad \text{for} \quad k > L+2. \tag{22}$$

$G_{\beta_1,L}(\xi)$ is singular at $\xi = 0$, hence the wavefunction of the radial part in the region $E > 0$ can be expressed as

$$R_1(\alpha_{1b}r) = C_{1b}\sum_{k=L+1}^{\infty} A_k^L(\beta_1)(\alpha_{1b}r)^{k-1} \tag{23}$$

where C_{1b} is the normalization constant.

(c) For zero energy $E = 0$. Substituting $E = 0$ into (6), one obtains

$$r^2\frac{\partial^2 R(r)}{\partial r^2} + 2r\frac{\partial R(r)}{\partial r} + \left(-L(L+1) + \frac{2\mu e^2}{\varepsilon\hbar^2}r\right)R(r) = 0. \tag{24}$$

Compared with the modified Bessel equation

$$r^2\frac{\partial^2 u(r)}{\partial r^2} + (1-2\omega)r\frac{\partial u(r)}{\partial r} + (\omega^2 - \nu^2\gamma^2 + \alpha^2\gamma^2 r^{2\gamma})u(r) = 0. \tag{25}$$

If we set $\omega = -1/2$, $\gamma = 1/2$, $\nu = 2L+1$, and $\alpha_{1c}^2 = 8\mu e^2/\varepsilon\hbar^2$, then the solution of (25) can be expressed as

$$u(\alpha_{1c}r) = r^{\omega}[C_{1c}J_{\nu}(\alpha_{1c}r^{\gamma}) + C_{1c}N_{\nu}(\alpha_{1c}r^{\gamma})] \tag{26}$$

where $J_{\nu}(\alpha_{1c}r^{\gamma})$ is the Bessel function and $N_{\nu}(\alpha_{1c}r^{\gamma})$ is the Neumann function. Since the radial function must be finite for $L = 0$, therefore, the wavefunction of the radial part can be written as

$$R_1(a_{1c}r) = C_{1c}r^{-1/2}J_{2L+1}\left(\sqrt{\frac{8\mu e^2}{\varepsilon\hbar^2}}r^{1/2}\right). \tag{27}$$

(II) For $\boldsymbol{a} \leqslant r < \boldsymbol{b}$, $V(r) = V_2$. The differential equation for the radial part $R(r)$ can be expressed as

$$-\frac{\hbar^2}{2\mu}\left(\frac{\partial^2}{\partial r^2} + \frac{2}{r}\frac{\partial}{\partial r} - \frac{L(L+1)}{r^2}\right)R(r) - \frac{e^2}{\varepsilon r}R(r) + V_2R(r) = ER(r). \tag{28}$$

Define $\alpha_2^2 = -8\mu(E - V_2)/\hbar^2 > 0$, $\xi = \alpha_2 r$, $\lambda_2 = 2\mu e^2/\varepsilon\hbar^2\alpha_2$ and $R(\xi) = \xi^{-1}W(\xi)$, Then (28) can be rewritten as

$$\frac{\partial^2 W}{\partial\xi^2} + \left(-\frac{1}{4} + \frac{\lambda_2}{\xi} + \frac{\frac{1}{4} - (L+\frac{1}{2})^2}{\xi^2}\right)W = 0. \tag{29}$$

This is the Whittaker equation. Thus, the solution can be written as

$$\begin{aligned}R_2(\alpha_2 r) = {} & C_{21}\mathrm{e}^{-\alpha_2 r/2}(\alpha_2 r)^L\Phi(L+1-\lambda_2, 2L+2, \alpha_2 r) \\ & + C_{22}\,\mathrm{e}^{-\alpha_2 r/2}(\alpha_2 r)^L\left\{\Phi(L+1-\lambda_2, 2L+2, \alpha_2 r)\ln(\alpha_2 r)\right. \\ & + \sum_{k=0}^{\infty}\frac{(L+1-\lambda_2)_k}{(2L+2)_k}\frac{(\alpha_2 r)^k}{k!}[\phi(L+1-\lambda_2+k) - \phi(2L+2+k) - \phi(1+k)] \\ & + \frac{\Gamma(2L+1)\Gamma(2L+2)\Gamma(-L-\lambda_2)(-1)^{2L+2}}{\Gamma(L+1-\lambda_2)} \\ & \left.\times\sum_{k=0}^{2L}\frac{(-L-\lambda_2)_k}{(-2L)_k}\frac{(\alpha_2 r)^{k-2L-1}}{k!}\right\}\end{aligned}$$

where C_{21}, C_{22} are normalization constants.

(III) For $r \geqslant \boldsymbol{b}$, $V(r) = V_3$. The differential equation for the radial part $R(r)$ can be expressed as

$$-\frac{\hbar^2}{2\mu}\left(\frac{\partial^2}{\partial r^2}+\frac{2}{r}\frac{\partial}{\partial r}-\frac{L(L+1)}{r^2}\right)R(r)-\frac{e^2}{\varepsilon r}R(r)+V_3R(r)=ER(r). \tag{30}$$

Define $\alpha_3^2 = -8\mu(E - V_3)/\hbar^2 > 0$, $\xi = \alpha_3 r$, $\lambda_3 = 2\mu e^2/\varepsilon\hbar^2\alpha_3$ and $R(\xi) = \xi^{-1}W(\xi)$. Then (30) becomes

$$\frac{\partial^2 W}{\partial \xi^2}+\left(-\frac{1}{4}+\frac{\lambda_3}{\xi}+\frac{\frac{1}{4}-(L+\frac{1}{2})^2}{\xi^2}\right)W=0. \tag{31}$$

This is the Whittaker equation. The Whittaker functions expressed in (9) and (10) are not well behaved as ξ becomes very large, we thus turn to use the integral representation of Whittaker function

$$W_{\lambda_3,L}(\xi) = C_3 \mathrm{e}^{-\xi/2}\xi^{\lambda_3}\int_0^\infty \mathrm{e}^{-t}t^{-\lambda_3+L}\left(1+\frac{t}{\xi}\right)^{\lambda_3+L}\mathrm{d}t \tag{32}$$

in our calculation. Hence the radial part of the wavefunction in the $r > \boldsymbol{b}$ region can be written as

$$R_3(\alpha_3 r) = C_3 \mathrm{e}^{-\alpha_3 r/2}(\alpha_3 r)^{\lambda_3-1}\int_0^\infty \mathrm{e}^{-t}t^{-\lambda_3+L}\left(1+\frac{t}{\alpha_3 r}\right)^{\lambda_3+L}\mathrm{d}t. \tag{33}$$

The boundary conditions require:

$$\frac{R_1'(\alpha_1 a)}{R_1(\alpha_1 a)} = \frac{R_2'(\alpha_2 a)}{R_2(\alpha_2 a)} \tag{34}$$

$$\frac{R_2'(\alpha_2 b)}{R_2(\alpha_2 b)} = \frac{R_3'(\alpha_3 b)}{R_3(\alpha_3 b)}. \tag{35}$$

Using the above two equations, one can obtain the eigenvalue E.

3. Results and discussion

In this work, we have calculated the ground and excited state energies of a hydrogenic impurity located at the centre of a multi-layered quantum dot for different confining potential energies and radius of the core and shell. To make a comparison, we first set $V_2 = V_3 = V$ which is equivalent to considering the case of a single-layered quantum dot. For a single-layered quantum dot with very large dot radius, the impurity behaves just like a 3D free hydrogen atom, thus its state energy will approach the 3D value $-1/n^2$ Ry, where n is the principal quantum number. If the dot radius decreases, the confinement effect enhances the state energy more prominently. Thus, the state energy of the impurity increases monotonically with the dot radius. However, as the dot radius is further decreased, the state energy of the impurity may become higher than the confining barrier. In the meanwhile, the kinetic energy of the confined electron becomes larger by uncertainty principle and thus increases the probability of the electron leaking outside the well.

Figure 1 shows the calculated ground state energy of a hydrogenic impurity located at the centre of a MLQD with $V_2 = V_3 = V$ as a function of dot radius for four different potential barriers. For an infinite potential barrier, as the dot radius decreases from infinite to zero, the impurity energy increases monotonically from -1 Ry to infinity. According to figure 1, one can see that the ground state energies are almost not influenced by the potential barrier height and they all approach -1 Ry as the dot radius is larger than $4a_0^*$. While the ground state

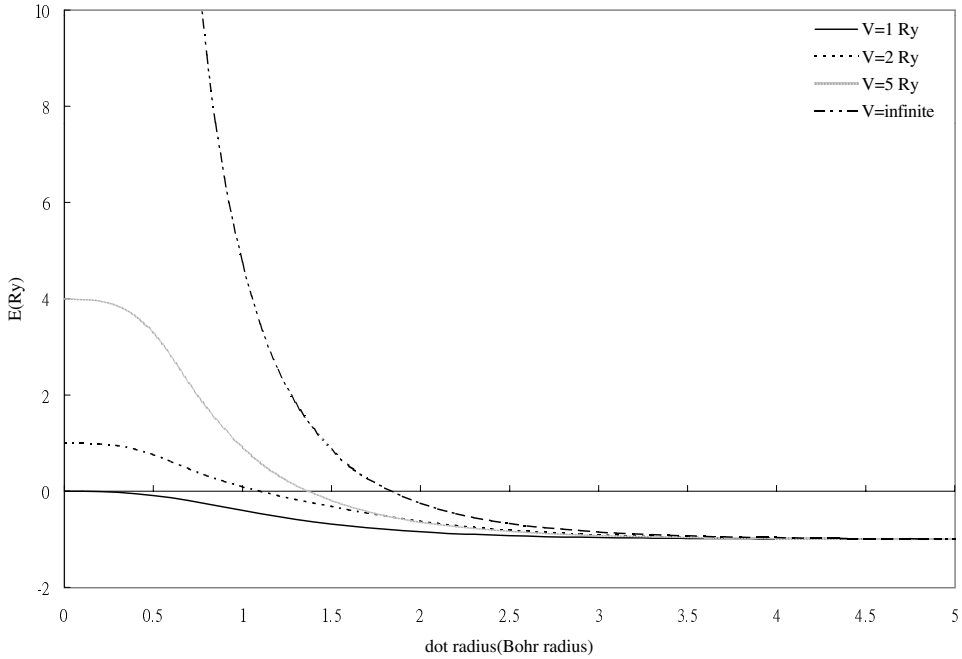

Figure 1. The ground state energy of a hydrogenic impurity in a single-layered QD as a function of dot radius with a potential barrier $V = 1$ Ry, 2 Ry, 5 Ry and infinity, respectively.

energies are influenced by the potential barrier as the dot radius decreases to a value less than $4a_0^*$. The ground state energy of the impurity located at the centre of a MLQD ($V_2 = V_3 = V$) with a finite height potential barrier approaches $(V - 1)$ Ry as the dot radius becomes zero. An electron bounded to an impurity at the centre of a QD never 'sees' the surface of the dot in a very large dot, and behaves as a 3D electron bounded to an impurity in the bulk of GaAs, thus the ground state energy approaches -1 Ry. For zero dot radius, the electron leaks outside the well and appears in the region of $Ga_{1-x}Al_xAs$, therefore it behaves as a 3D electron bounded to an impurity in the bulk of $Ga_{1-x}Al_xAs$ and the ground state energy approaches $(V - 1)$ Ry. Therefore, our results for the multi-layered QD can be successfully reduced to the single-layered QD case as we set $V_2 = V_3$.

Now consider the multi-layered quantum dot ($V_2 \neq V_3$). Figure 2 shows the ground state energy of an impurity in a multi-layered QD with $V_3 = 5$ Ry, $\boldsymbol{b} = 24a_0^*$ for various potential barriers V_2. According to figure 2, as the core radius approaches infinity, the ground state energy approaches -1 Ry, which is the same as the result of single-layered QD. One can see that the ground state energy approaches V Ry as the dot radius approaches zero, where $V = V_2 - 1$ if $V_2 - 1 < V_3$, and $V = V_3$ if $V_2 - 1 > V_3$. This means that the electron leaks out as the core radius reduces to some characteristic value, and finally stays in the region with a smaller potential barrier in the multi-layered QD. The ground state energy increases as the core radius decreases, and it attains a characteristic value E_0 as the radius reduces to zero. In the case of a single-layered QD, the E_0 is equal to $(V - 1)$ Ry,where V is the potential barrier height. In the case of a multi-layered QD, the value of E_0 depends on the value of $(V_2 - V_3)$ and the shell thickness $\boldsymbol{b} - \boldsymbol{a}$. As the core radius $\boldsymbol{a}$ is reduced to zero, the electron leaks out of the core dot and tunnels to the shell region ($\boldsymbol{a} \leqslant r < \boldsymbol{b}$) for $V_2 - 1 < V_3$ or to the bulk region ($r \leqslant \boldsymbol{b}$) for $V_2 - 1 > V_3$. If the electron tunnels to the shell region with a large shell thickness,

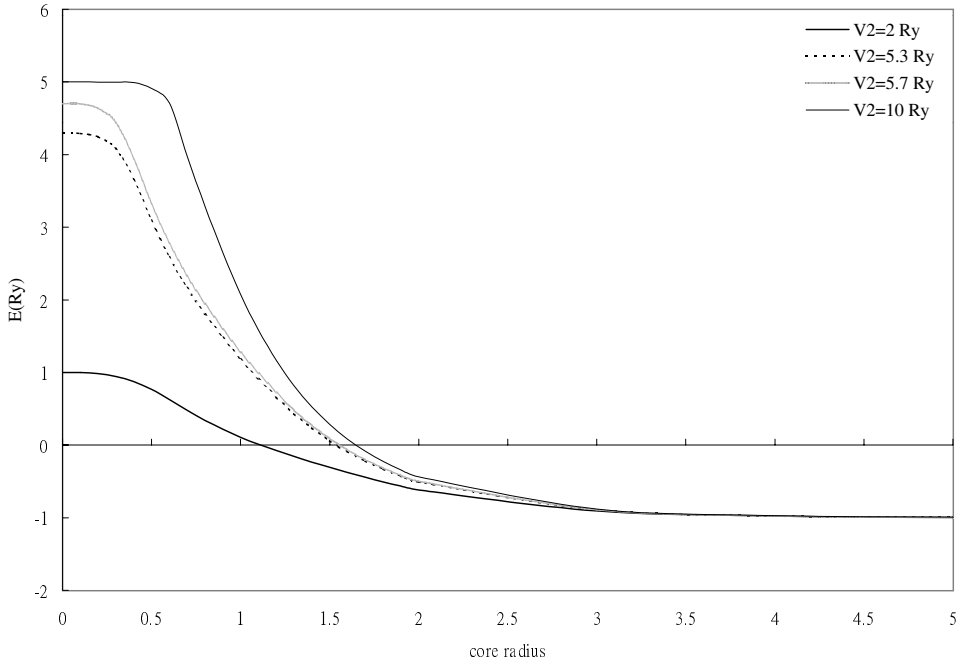

Figure 2. The ground state energy of electron in multi-layered QD with impurity as a function of core radius for $\boldsymbol{b} = 24a_0^*$, the shell potential $V_3 = 5$ Ry and $V_2 = 2$ Ry, 5.3 Ry, 5.7 Ry and 10 Ry, respectively.

the ground state energy (E_0) of the electron becomes ($V_2 - 1$). It behaves like the case of a single-layered quantum dot with potential barrier equal to V_2 as the radius reduces to zero. If the electron tunnels to the bulk region with a large shell thickness, then the ground state energy of the electron becomes V_3. In this case, the electron behaves just like a free electron in the bulk without the binding of the impurity.

Figure 3 shows the ground state energy of a hydrogenic impurity in multi-layered QD as a function of core radius with $V_2 = 2$ Ry and $V_3 = 1$ Ry for various shell thicknesses $(\boldsymbol{b} - \boldsymbol{a}) = 0.1, 0.5, 1, 2a_0^*$, respectively. For large core radius, the impurity inside the multi-layered QD behaves like a free hydrogen atom even though the shell thickness is different. As the core radius decreases, the energy increases monotonically until it attains a maximum value, and then decreases monotonically to certain limiting value as the core radius approaches zero as shown in figure 3. The limiting value depends on the shell thickness. This is because the tunnelling probability of the electron depends on the shell thickness for small dot radius. As the thickness of the shell decreases, the probability of tunnelling to the bulk region increases and the maximum value of the state energy decreases. One can note from figure 3, that the probability of electron tunnelling increases as the shell thickness decreases.

Figure 4 shows the ground state energy of a hydrogenic impurity in a multi-layered QD as a function of core radius with $V_2 = 2$ Ry and the shell thickness is kept as $(\boldsymbol{b} - \boldsymbol{a}) = 1a_0^*$ for various V_3. For a small radius, the effect of the height of the bulk potential barrier is more important. From figure 4, one can note that the maximum value of the state energy for the case of $V_3 = 1.5$ Ry is larger than that of $V_3 = 1$ Ry. Thus the height of the bulk potential barrier influences the electron tunnelling as the core radius is small. Figure 5 shows the ground state energy of a hydrogenic impurity in the multi-layered QD as a function of total dot radius with

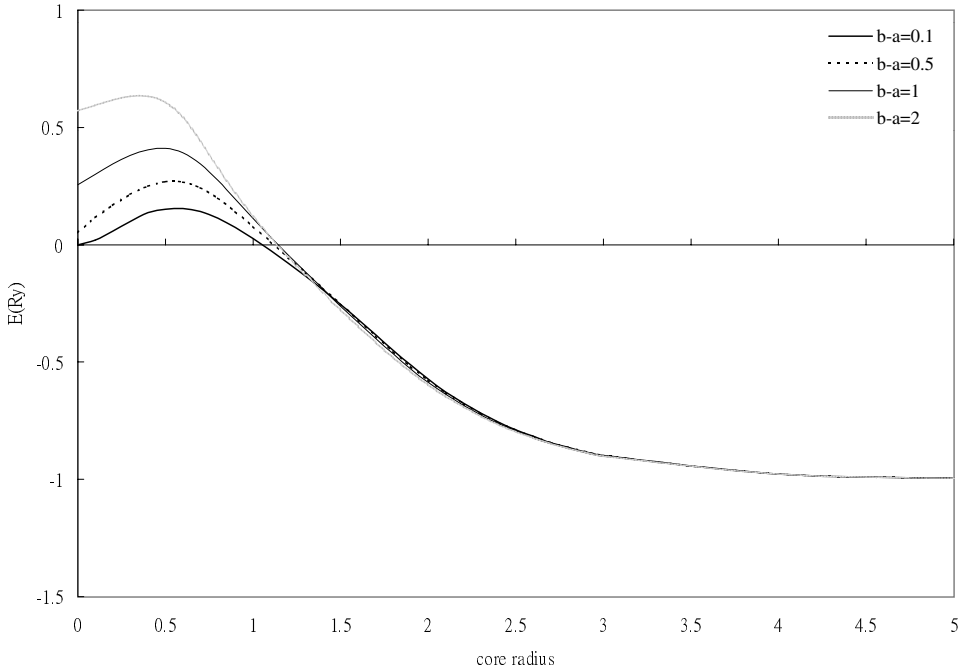

Figure 3. The ground state energy of a hydrogenic impurity in multi-layered QD as a function of core radius with $V_2 = 2$ Ry and $V_3 = 1$ Ry for various thickness of shell $(\boldsymbol{b} - \boldsymbol{a}) = 0.1$, 0.5, 1, $2a_0^*$, respectively.

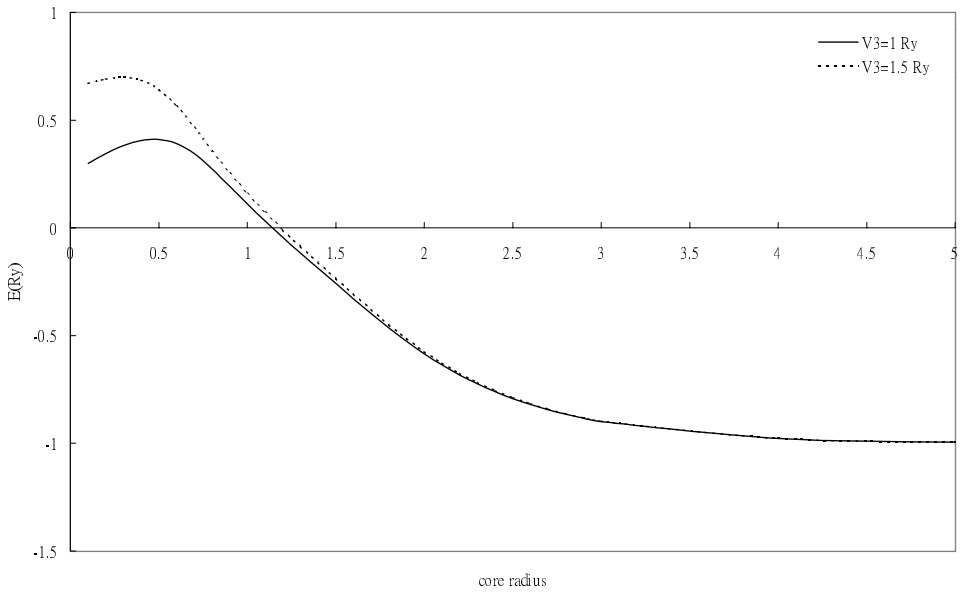

Figure 4. The ground state energy of a hydrogenic impurity in multi-layered QD as a function of core radius with $V_2 = 2$ Ry and $(\boldsymbol{b} - \boldsymbol{a}) = 1a_0^*$ for various $V_3 = 1$ Ry, 1.5 Ry, respectively.

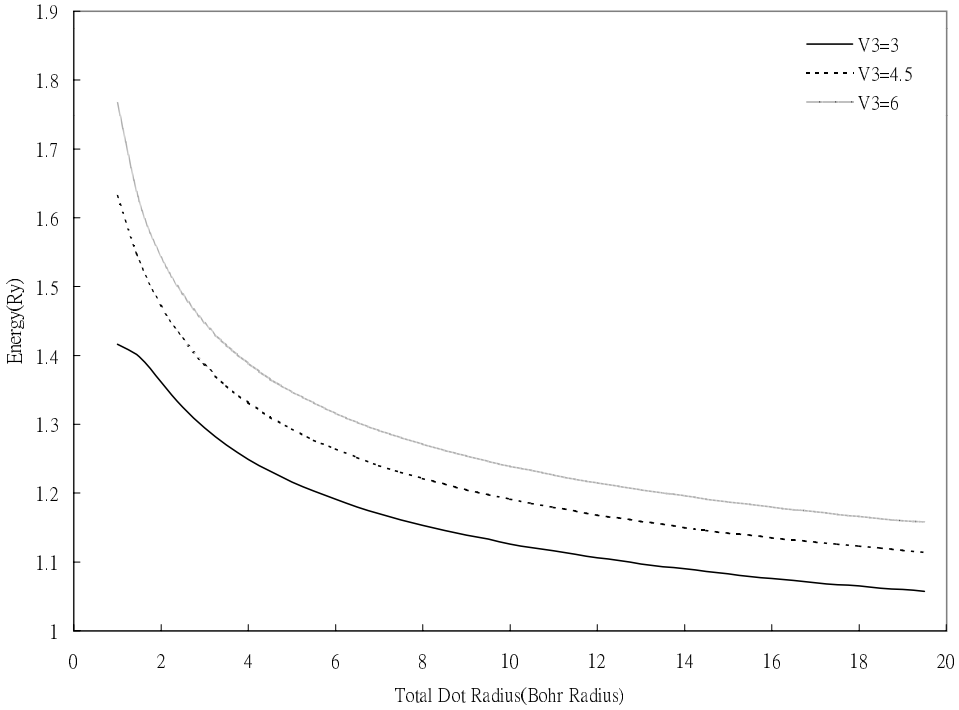

Figure 5. The ground state energy of a hydrogenic impurity in multi-layered QD as a function of total dot radius with $V_2 = 5$ Ry and $\boldsymbol{a} = 1a_0^*$ for various $V_3 = 3$ Ry, 4.5 Ry and 6 Ry, respectively.

$V_2 = 5$ Ry and $\boldsymbol{a} = 1a_0^*$ for various V_3. The ground state energy increases monotonically as the total dot radius decreases when the core radius is kept constant. From figure 5, one can see that the curve of $V_3 = 6$ Ry is steeper than that of $V_3 = 3$ Ry as the core radius is small. Figure 6 shows the 1s-, 2p-, 3d- and 4f-state energies of a hydrogenic impurity in the single-layered QD (GaAs–$Ga_{1-x}Al_xAs$) as functions of dot radius with the Al concentration $x = 0.1$. For Al concentration $x = 0.1$, the potential of $Ga_{1-x}Al_xAs$ is equal to 16.787 Ry. According to figure 6, as the dot radius approaches infinity, the 1s-state energy approaches -1 Ry; the 2p-state energy approaches -0.25 Ry; the 3d-state energy approaches -0.11 Ry; the 4f-state energy approaches -0.067 Ry. For a single-layered quantum dot with very large dot radius, the impurity behaves just like a 3D free hydrogen atom, thus its state energy will approach the 3D value $-1/n^2$. According to figure 6, as the dot radius is reduced to zero, the 1s-state energy approaches $(16.787 - 1) = 15.787$ Ry; the 2p-state energy approaches $(16.787 - 0.25) = 16.537$ Ry; the 3d-state energy approaches $(16.787 - 0.111) = 16.676$ Ry; the 4f-state energy approaches $(16.787 - 0.067) = 16.72$ Ry. Summarily, as the dot radius reduces to zero, the excited state energies approach $(V - 1/n^2)$ Ry. Our results are all in agreement with the limiting value for both large and small dot radii. Figure 7 shows the 1s-, 2p-, 3d- and 4f-state energies of a hydrogenic impurity in the multi-layered QD (GaAs–$Ga_{1-x}Al_xAs$–$Ga_{1-y}Al_yAs$) as functions of core radius with the Al concentration $x = 0.2$ and $y = 0.1$, and $\boldsymbol{b} = 10a_0^*$. The curves shown in figure 7 and figure 6 are very similar. But the excited state energies of impurity in the QD is also dependent on the potential barrier height, the thickness of shell and the difference of shell potential and bulk potential, like the case of the ground state energy.

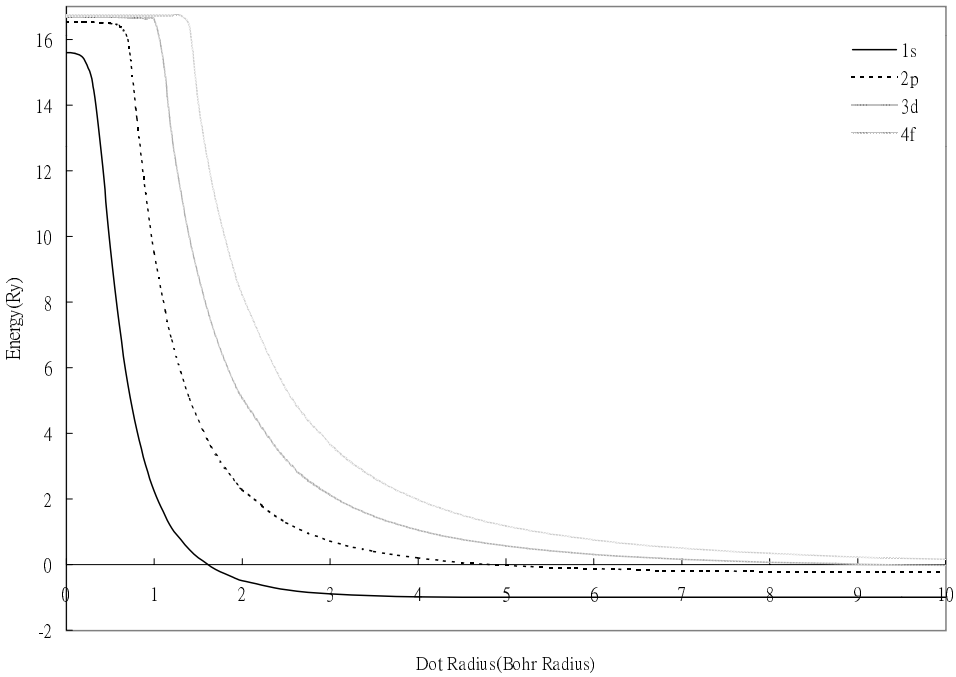

Figure 6. 1s-, 2p-, 3d-, 4f-state energies of a hydrogenic impurity in the single-layered QD (GaAs–$Ga_{1-x}Al_xAs$) as functions of dot radius with the Al concentration $x = 0.1$.

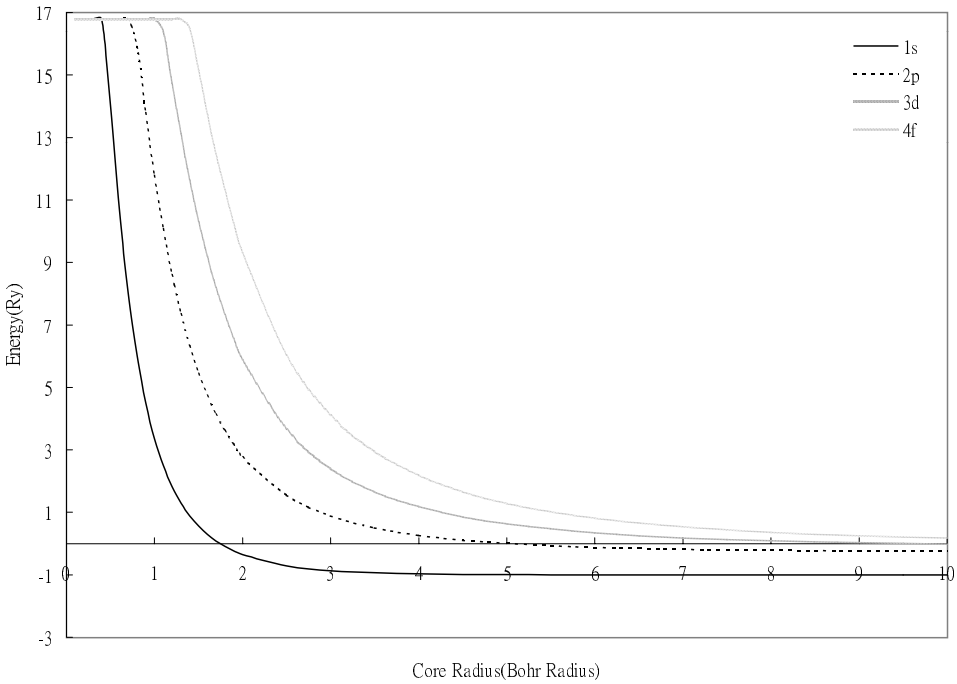

Figure 7. 1s-, 2p-, 3d-, 4f-state energies of a hydrogenic impurity in the multi-layered QD (GaAs–$Ga_{1-x}Al_xAs$–$Ga_{1-y}Al_yAs$) as functions of core radius with the Al concentration $x = 0.2$ and $y = 0.1$, and $\boldsymbol{b} = 10a_0^*$.

From the above results, one can note that the state energy behaviours for the impurity located at the centre of the MLQD and at the centre of the single-layered quantum dot are very similar for large core radius. For small core radius, the state energies for both cases also exhibit similar features. However, the limit values of the state energies for small core radius depend on the energy difference between the barrier height of the values V_2 and V_3. Brown and Spector [9] and Zhu and Chen [22] calculated the binding energies of an off-centre donor in QWs and QDs, respectively. They showed that the binding energies decrease and the level ordering changes as the impurity location shifts to the edge or out of the QDs and QWs. Therefore, one may expect that in the case of an off-centre impurity for a MLQD system, the state energies might also decrease and the level ordering might change as the impurity location is shifted to the edge of the MLQD.

4. Conclusion

We have calculated the ground state and excited state energies of a hydrogenic impurity in a multi-layered QD which consists of a spherical core coating with a spherical shell (potential barrier V_2) and embedded in a bulk material (potential barrier V_3). Our MLQD model can be reduced successfully to the case of single layer QD if we set $V_2 = V_3$. The results for a single-layered QD are in agreement with the limiting values. Our calculation shows that as the dot radius becomes very large, the state energy of an impurity in a MLQD approaches $-1/n^2$ and thus behaves like that in a single-layered QD. However, as the dot radius approaches zero, the behaviour of the impurity in the MLQD is very different from that in the single-layered QD. In the single-layered QD, the state energies approach $(V - 1/n^2)$ Ry, $n = 1, 2, 3, \ldots$ as the dot radius is reduced to zero, and behaves just like a free hydrogen atom in the bulk material. While in the multi-layered QD, as the core radius reduces to zero, the state energies approach $(V_2 - 1/n^2)$, $n = 1, 2, 3, \ldots$ or V_3 Ry. The limiting values depend on the difference between the barrier height of the shell potential (V_2) and that of the bulk potential (V_3).

Acknowledgments

This work is supported partially by Deh Yu College of Nursing Management and partially by the National Science Council, Taiwan under the grant number NSC 88-2112-M-009-004 R.O.C.

References

[1] Fukui T, Ando S and Tokura Y 1991 *Appl. Phys. Lett.* **58** 2018
[2] Fang H, Zeller R and Stiles P J 1989 *Appl. Phys. Lett.* **55** 1433
[3] Smith T P III, Lee K Y, Knoedler C M, Hong J M and Kern D P 1988 *Phys. Rev.* B **38** 2172
[4] Reed M A, Randall J N, Aggarwal R J, Matyi R J, Moore T M and Wetsel A E 1988 *Phys. Rev. Lett.* **60** 535
[5] Ye Q, Tsu R and Hicollian E H 1991 *Phys. Rev.* B **44** 1806
[6] Bastard G 1981 *Phys. Rev.* B **24** 4714
[7] Montenegro N P, Lòpez-Gondar J and Oliveira L E 1991 *Phys. Rev.* B **43** 1824
[8] Masselink W T, Chang Y C and Morkoc H 1983 *Phys. Rev.* B **28** 7373
[9] Brown J W and Spector H N 1986 *J. Appl. Phys.* **59** 1179
[10] Bryant G W 1985 *Phys. Rev.* B **31** 7812
[11] Bryant G W 1984 *Phys. Rev.* B **29** 6632
[12] Miller R C, Gossard A C, Tsang W T and Munteanu O 1982 *Phys. Rev.* B **25** 3871
[13] Branis S V, Li G and Bajaj K K 1993 *Phys. Rev.* B **47** 1316
[14] Chuu D S, Hsiao C M and Mei W N 1992 *Phys. Rev.* B **46** 3898
[15] Hsiao C M, Mei W N and Chuu D S 1992 *Solid State Commun.* **81** 807

[16] Nair S V, Ramaniah L M, and Rustagi K C 1992 *Phys. Rev.* B **45** 5969
[17] Einevoll G T and Chang Y C 1989 *Phys. Rev.* B **40** 9683
[18] Kumar A, Laux S E and Stern F 1990 *Phys. Rev.* B **42** 5166
[19] Porras-Montenegro N and Pérez-Merchancano S T 1992 *Phys. Rev.* B **46** 9780
[20] Zhu J L, Zhao J H, Duan W H and Gu B L 1992 *Phys. Rev.* B **46** 7546
[21] Zhu J L, Xiong J J and Gu B L 1990 *Phys. Rev.* B **41** 6001
[22] Zhu J L and Chen X 1994 *Phys. Rev.* B **50** 4497
[23] He X F 1991 *Phys. Rev.* B **43** 2063
[24] Bose C and Sarkar C K 2000 *Phys. Status Solidi* b **218** 461
[25] Bose C 1999 *Physica* E **4** 180
[26] Bose C and Sarkar C K 1998 *Solid-State Electron.* **42** 1661
[27] Bose C and Sarkar C K 1998 *Physica* B **253** 238
[28] Betancur F J, Mikhailov I D and Oliveira I E 1998 *J. Phys. D: Appl. Phys.* **31** 3391
[29] Mikhailov I D and Betancur F J 1999 *Phys. Status Solidi* b **213** 325
[30] Betancur F J, Mikhailov I D and Sierra J 1998 *Phys. Status Solidi* b **208** 51
[31] Betancur F J and Mikhailov I D 1995 *Phys. Rev.* B **51** 4982
[32] Kash K, Scherer A, Worlock J M, Graighead H G and Tamargo M C 1986 *Appl. Phys. Lett.* **49** 1043
[33] Skromme B J, Bhat R and Koza M A 1988 *Solid State Commun.* **66** 543
[34] Temkin H, Dolan G J, Panish M B and Chu S N G 1987 *Appl. Phys. Lett.* **50** 413
[35] Shanabrook B V, Comas J, Perry T A and Merlin R 1984 *Phys. Rev.* B **29** 7096
[36] Gammon D, Merlin R, Maselink W T and Morkoc H 1986 *Phys. Rev.* B **33** 2919
[37] Chaudhuri S 1983 *Phys. Rev.* B **28** 4480
[38] Lane P and Greene R L 1986 *Phys. Rev.* B **33** 5871
[39] Schooss D, Mews A, Eychmüller A and Weller H 1994 *Phys. Rev.* B **49** 17 072
[40] Eychmüller A, Mews A and Weller H 1993 *Chem. Phys. Lett.* **208** 59
[41] Mews A, Eychmüller A, Giersig M, Schooss D and Weller H 1994 *J. Phys. Chem.* **98** 934
[42] Mews A, Kadavaich A V, Banin U and Alivisatos A P 1996 *Phys. Rev.* B **53** R13 242
[43] Kido J, Hongawa K, Okuyama K and Nagai K 1993 *Appl. Phys. Lett.* **63** 2627
[44] Hu B, Yang Z, and Karasz F E 1994 *J. Appl. Phys.* **76** 2419
[45] Dabbousi B O, Bawendi M G, Onitsuka O and Rubner M F 1995 *Appl. Phys. Lett.* **66** 1316
[46] Tsu R and Babić D 1994 *Appl. Phys. Lett.* **64** 1806
[47] Lannoo M, Delerue C and Allan G 1995 *Phys. Rev. Lett.* **74** 3415
[48] Proetto C R 1996 *Phys. Rev. Lett.* **76** 2824
[49] Adachi S 1985 *J. Appl. Phys.* **58** R1
[50] Jeffrey A, Ryzhik I, Gradshteyn I, Geronimus Yu and Tseytlin M 1980 *Table of Integrals, Series and Products* (New York: Academic) p 1059
[51] Arfken G 1973 *Mathematical Methods for Physicists* 2nd edn (New York: Academic) p 639
[52] Abramowitz A and Stegun I A 1964 *Handbook of Mathematical Function with Formulae, Graphs and Mathematical Tables (Natl Bureau Stand. Appl. Math. Series 55)* (Washington, DC: US GPO) p 538